2024 IEEE International Conference on Robotics and Automation (ICRA 2024)
May 13-17, 2024. Yokohama, Japan

AeroDima: Cheetah-Inspired Aerodynamic Tail Design for Rapid Maneuverability

Daryn Bright[1], Stacey Shield[1], and Amir Patel[1], *Senior Member, IEEE*

***Abstract*— Scientists have long theorized that the cheetah's tail contributes to its impressive maneuvrability at high speeds by stabilizing its body. This has inspired the design of several agile robots, including *Dima* - a wheeled platform that used cheetah-inspired inertial tail swings to better execute rapid acceleration and turning motions. Subsequent research suggests that the effectiveness of the cheetah's tail might be enhanced by aerodynamic effects. In this paper, we introduce *AeroDima*: a follow-up to the original *Dima* design that uses aerodynamic drag on the tail as the primary mechanism for generating the stabilizing torque. The resulting sail-like tail is substantially lighter than the original, but still improves the performance of the platform, allowing it to enter turns at a higher speed without toppling. While the yaw rate of the robot was actually higher without the tail, the tail substantially reduced unwanted roll, confirming that this appendage increases maneuvrability by increasing stability, rather than by directly contributing to lateral acceleration.**

I. Introduction

Cheetahs, known for their exceptional high-speed maneuvers, can reach speeds of up to 29 m/s and accelerate at rates up to 7.5 m/s^2, with their tail playing a crucial role in maintaining stability during these rapid movements [1], [2]. Inspired by this, our research focuses on replicating such agility in robotic platforms, particularly through the implementation of an aerodynamic tail, diverging from prior emphasis on inertial effects [3], [4]. Despite initial designs being modeled on the assumption of a heavier tail, further anatomical studies revealed the cheetah's tail to be lighter, prompting an investigation into aerodynamic contributions, which identified significant aerodynamic torque due to its large surface area [5].

This paper introduces *AeroDima* (Fig. 1), an evolution of the *Dima* platform, now incorporating a dynamic aerodynamic tail designed for enhanced maneuverability without the compromise of increased mass. Unlike existing models primarily utilizing inertial tails for stabilization (e.g., *MSU Tailbot*, *MIT Cheetah*, *Berkeley Tailbot*, *Dima I* and *Dima II* [3], [5]–[8]), *AeroDima*, alongside *Minitaur* and *SailRoACH* [9], [10], explores aerodynamics as a primary mechanism for stabilization. Our approach differs in actively utilizing the tail's movement in conjunction with the body's velocity to achieve stabilization, surpassing the limitations of previous designs that either employed the tail as a static rudder or did not fully explore dynamic effects.

*This work was supported by the National Research Foundation (NRF) of South Africa grant number 137762.

[1] Authors are with the Department of Electrical Engineering at the University of Cape Town at the University of Cape Town, South Africa. Corresponding Author: BRGDAR004@myuct.ac.za

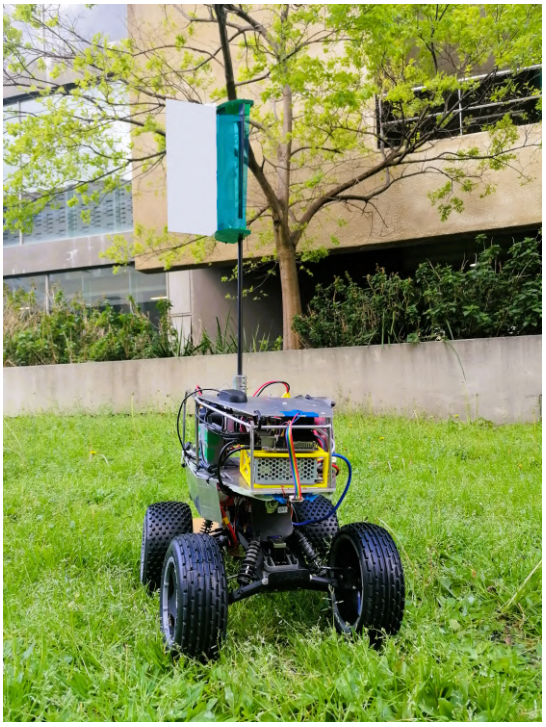

Fig. 1: *AeroDima*, the high-speed actuated aerodynamic tailed robot.

To validate the effectiveness of a lightweight aerodynamic tail, we compared its angular impulse during a pitch tail swing against that of an inertial tail across various speeds (Fig. 2). Our findings reveal that even the lightest aerodynamic tail provides comparable stabilization to an inertial tail within the operational speed range of *Dima*, showcasing the potential of aerodynamic tails in significantly reducing mass while maintaining maneuverability.

Drawing inspiration from the cheetah, our study not only reaffirms the significance of aerodynamic forces in high-speed maneuverability but also introduces a more sophisticated tail design with two actuated degrees of freedom, extending beyond the capabilities of previously studied 1-DOF aerodynamic tails.

II. Cheetah Tail Experiments

Improving the scientific understanding of the aerodynamic properties of the cheetah's tail was an important aim of this research. The objective of these preliminary experiments was to determine whether a quasi-steady state model (QSS) would be viable for dynamic movement of the tail as it had only been studied for static positioning [5].

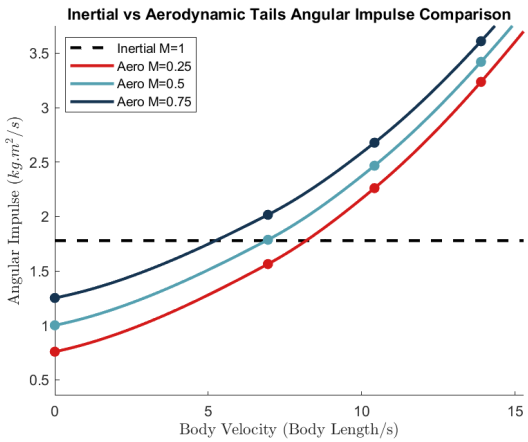

Fig. 2: Simulation showing at what forward velocity an aerodynamic tail, with a certain mass relative to the inertial tail, would outperform the inertial tail in terms of angular impulse experienced for a pitch swing.

Fig. 3: (Left) The three cheetah tails studied. (Right) A cheetah tail in the wind tunnel.

Three cheetah tails were obtained through a routine necropsy from the National Zoological Gardens in South Africa [5] and were attached to a steel threaded rod. These were each put onto an actuated rig with a Axia80-M20 6-axis force sensor to allow for data collection. The three tails and the wind tunnel can be seen in Fig. 3.

Two experiments were done: a static set and a dynamic set. In the static set, the tails were set to regular intervals of 15 ° ranging from 0 ° to 75 ° with the wind tunnel being set to produce wind speeds of 10, 20, and 30 m/s. In the dynamic set, the tails were set to swing from 90 ° to vertical down to produce an acceleration term.

The data logged from these experiments was put into a Euler-Lagrangian dynamics model, not described in this paper, and analyzed to produce the drag and lift coefficients of the cheetah tail for a QSS model. The added mass effect [11], effectively an air mass, was also considered. Fig. 4 shows the position profile of an experimental swing with the profiles of the simulated QSS and QSS with added mass models. An added mass effect was seen to be useful at certain velocities but was not a constant term, as the effect would change depending on the relative wind velocity. It has been seen in other studies [12] that there is a time-dependent term associated with aerodynamics, which will be explored in future work.

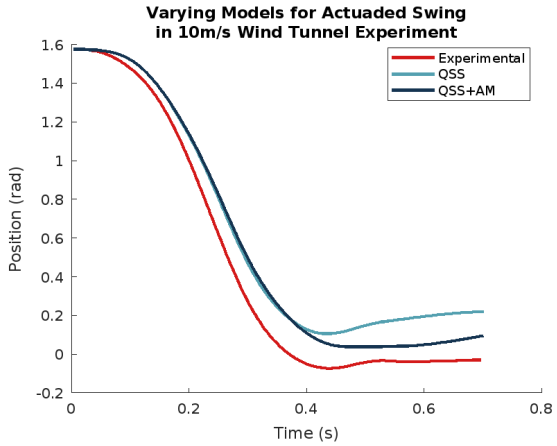

Fig. 4: The experimental versus simulated models of the cheetah swing in the wind tunnel at 10 m/s, showing that added mass can be beneficial at certain velocities.

III. Mechatronic Design

Building on our previous findings, this section outlines the development of a bio-inspired, aerodynamically efficient tail and the overall mechatronic design of the robotic platform.

A. Tail Design

Leveraging the freedom offered by robotics, unlike the constraints found in natural biology, we aimed to create a tail that, while lightweight, could harness significant aerodynamic forces. Drawing inspiration from the cheetah's efficient tail design and informed by aerodynamic principles, we developed eight tail prototypes. These designs were influenced by a variety of aerodynamic shapes sourced from established literature [9], [13], [14] and modeled in SolidWorks. Their performance was evaluated using SolidWorks' flow simulation feature, which employs a Computational Fluid Dynamics (CFD) solver for optimizing and calculating various aerodynamic parameters. The comparative analysis of these designs, based on their drag coefficients at different wind speeds (10, 20, and 30 m/s) and angles of attack (ranging from 0 ° to 75 ° in 15 ° increments), is presented in Fig. 5.

The drag and lift coefficients for each tail shape were calculated using the following equation:

$$C_D = \frac{2 * F_A}{\rho * A * {v_{wind}}^2}, \tag{1}$$

where C_D represents the drag coefficient, which was instrumental in identifying the most aerodynamically effective tail design.

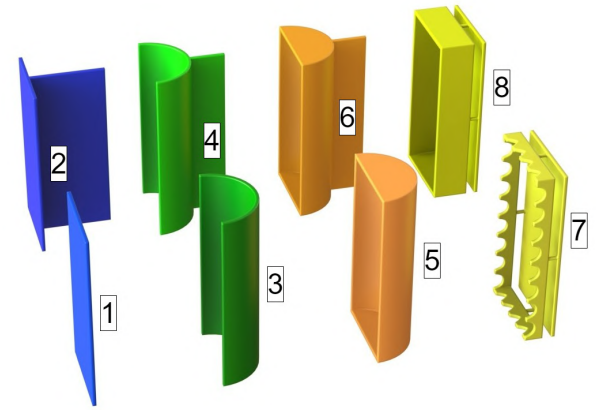

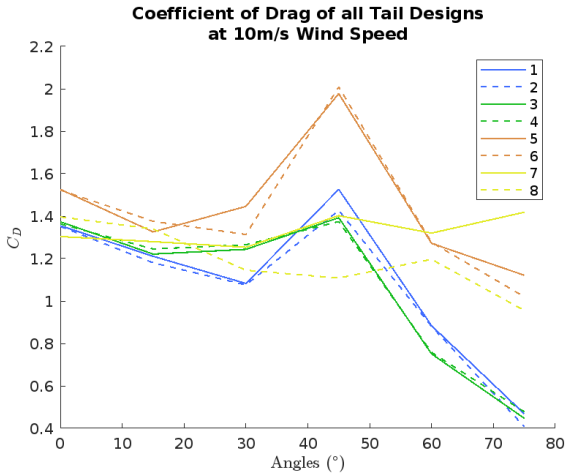

Fig. 5: (Top) Eight tail designs compared. (Bottom) The drag coefficients of the 8 analysed shapes from 0 ° to 75 ° at a wind speed of 10 m/s.

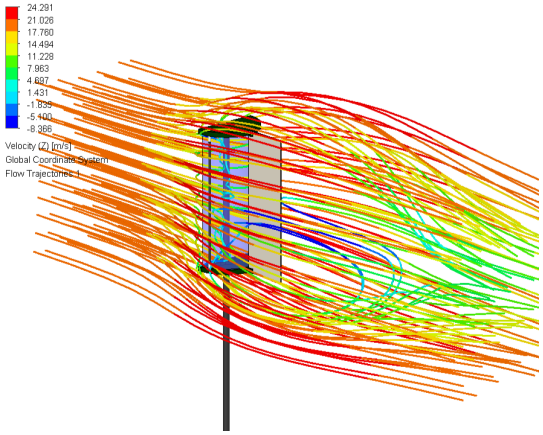

Fig. 6: Flow trajectory of the final design at a wind speed of 20 m/s.

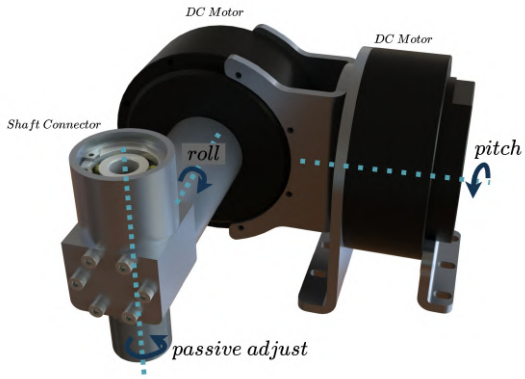

Fig. 7: The gearbox design with a 3-DOF underactuated system, with two DC motors actuating the pitch and roll axes. The third DOF is the passive axial rotation of the tail.

The design found to produce the largest drag coefficients was the half cylinder with end caps and backing board design (shape No. 6 in Fig. 5). This design was then made into a lightweight tail prototype with a carbon fibre shaft, aluminium joiners, PLA end caps, hard paper backing board, and a plastic film for the central cylinder, as also modeled in the simulation. The center of pressure was designed to be behind the center of rotation, as the tail was designed to have an unactuated degree of freedom that allowed the rotation of the tail to face into the highest relative wind velocity. This prototype was also analysed to determine the drag characteristics of the final design. A flow simulation velocity flow graph can be seen in Fig. 6.

The tail was attached to a differential gearbox with two AK70 T-Motors motors actuating the pitch and roll axes, however, only the actuated roll motion was performed in the preliminary experiments shown in this paper. The third, unactuated DOF came from the shaft connector that allowed the tail to passively adjust to point the tail to facing the total wind velocity vector. This motor gearbox configuration can be seen in Fig. 7.

B. Platform Design

The robotic platform used the Traxxas Stampede R/C as the base, as did the previous platform *Dima* II. The drive motor chosen was a sensored Hobbywind Xerun G3 2250kV DC motor, and the servo motor was a CL-380 38Kg Servo powered through a Hobbywing UBEC 10A for a steady power supply. Two AK70-10 Brushless DC Motors were used for tail actuation. The robot employed the following key sensors: the C94-M8P GPS unit, the BNO055 9-DOF IMU, the AEAT-6010-A05 Rotary Encoder.

The platform was controlled through an Nvidia Jetson Nano and a Teensy 4.0 microcontroller. Wireless commands were sent via an RF transceiver, by an external computer running a GUI to operate the vehicle. The embedded system design combining these components is included in Fig. 8. All the sensing and computing electronics, as well as the batteries, were mounted on the top plate of the platform. For added protection, a roll cage was added to protect the electronics as well as a 2 mm aluminium plate in certain areas to protect components from piercing damage. This can be seen in Fig. 1.

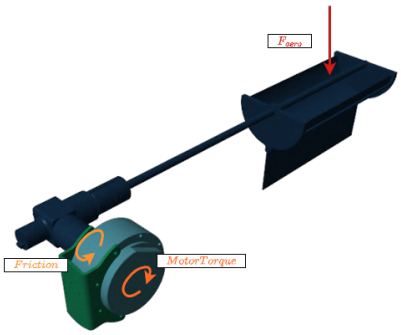

Fig. 9: Simscape model showing the aerodynamic force, the friction, and the motor input torque.

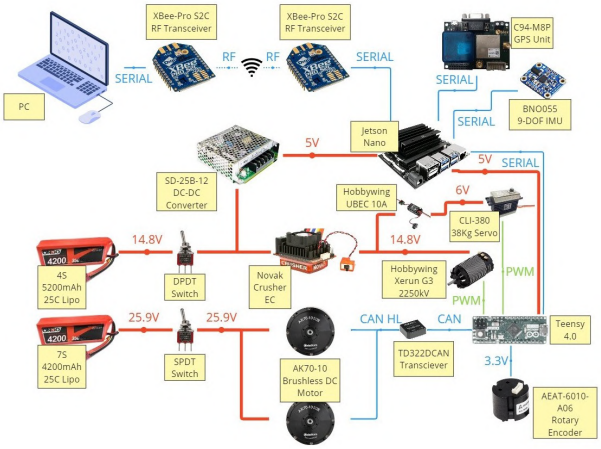

Fig. 8: Holistic overview of the embedded system of *AeroDima*.

IV. Modelling and Simulation

A. Aerodynamic Modelling

The tail, once manufactured, was put through the same wind tunnel dynamic tests as the cheetah tails were to determine the aerodynamic model of the final design to use for the simulation developed in MATLAB's physical modelling package Simscape. The tail's assembly was taken directly from the SolidWorks model, including all masses and inertias. Three forces were modelled to compare the Simscape model to the experiment: the aerodynamic forces, the friction, and the input torque. The torque was measured from the experiment and substituted into the model, while the coulomb and viscous friction coefficients were determined using unactuated swing motions and Cf and Vf were found to be 0.161 and 0.057 respectively.

The aerodynamic drag coefficients were found using this model. They varied across the various relative wind velocities that were experienced by the tail. The drag coefficients found through the experiment can be seen in Fig. 10. With these results, the line of best fit and a constant value model was compared and, due to the accuracy at the lower winds, as seen was similar to the cheetah tails, and the simplicity, a constant C_D of 2 was used.

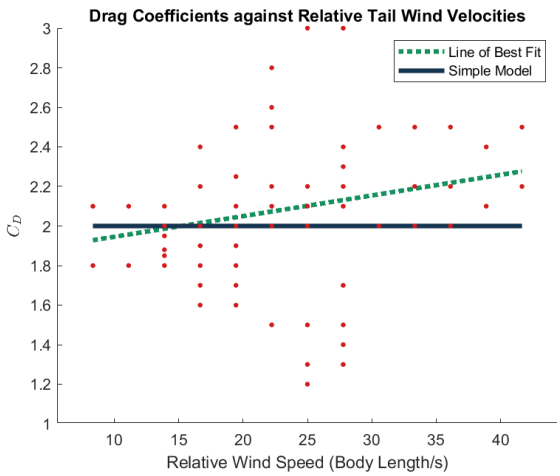

Fig. 10: Scatter plot of drag coefficients found from dynamic swings showing the line of best fit and the constant model

B. Physical Modelling

The platform was modelled in MATLAB's Simscape environment. This combined the tail model with a model of a four-wheeled vehicle capable of 6-DOF motion. This model was made to test the vehicle's metrics with and without the tail before implementing the same tests on *AeroDima*. All multibody models used were taken from the SolidWorks model.

The values of other key parameters were determined experimentally. For the spring-damping constants, each wheel and spring was attached to the end of a boom mechanism with displacement measurement sensors. These were then pressed down onto a force plate with an Axia80-M20 force sensor to measure the force against displacement graphs to determine the spring constant for each item. Through this test, the spring constant was determined to be 14806.

The range of speeds for the simulated vehicle was determined by measuring the velocity of the *AeroDima* platform driving in a straight line at throttle rates of up to 60%.

V. Experiments

The performance of the aerodynamic tail was compared to the baseline performance of the platform without the tail through a turning test in simulation and experimentally. The platform was set to drive at a certain speed and perform a turn once it had reached that speed. This turning maneuver was executed by the servo motor turning the front wheels at 30% for 0.5 s. Because of the delay of 0.14 s to complete the turn of the wheels, this ended up resulting in a 0.64 s duration from when the turn was initiated to when the wheels returned to the forward position. The speed was increased until the vehicle could no longer perform the turning maneuver without flipping over, meaning that the given configuration had reached its maneuvrability limit. This was turning procedure was imitated in the simulation. For all simulations, all sensors were logged at 1000 Hz, while for the physical experiments, the GPS was logged at

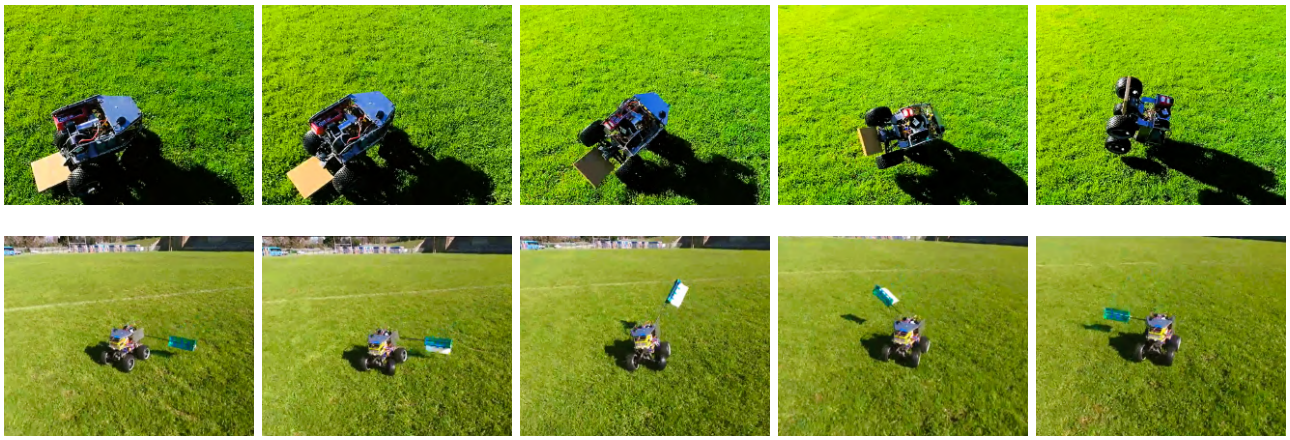

Fig. 11: (Top) *AeroDima* operating at its fastest tailless speed at **3.61** m/s. (Bottom) *AeroDima* operating its fastest recorded tailed flick at **6.10** m/s.

TABLE I
RESULTS

Metric	Sim Tailless	Sim Tailed	Exp Tailless	Exp Tailed
Speed ($Body\ Length/s$)	9.17	12.11	9.08	16.94
Max Yaw Rate (rad/s)	2.17	1.24	1.91	1.98
Avg. Yaw Rate (rad/s)	1.46	0.85	1.24	0.70
Max Lin Acc (m/s^2)	5.01	6.04	4.79	5.16
Avg. Lin Acc (m/s^2)	3.70	3.40	3.27	2.01
Max Maneuv. ($\frac{\dot{\theta}m}{s^2}$)	413.31	304.66	366.82	692.57
Avg. Maneuv. ($\frac{\dot{\theta}m}{s^2}$)	276.06	213.67	237.94	245.34
Int. of Roll Rate (rad)	932.43	435.92	25.43	15.98

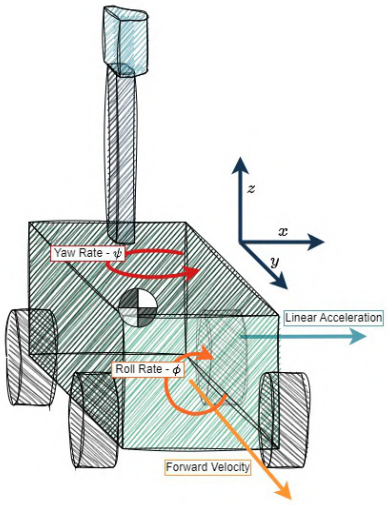

Fig. 12: The metrics illustrated on representation of *AeroDima*.

10 Hz, and the IMU and tail encoder at 100 Hz. Several tail flick speeds were trialled for the tests with the tail, with the best performance occurring when the tail was swung at 8 rad/s. For brevity, only the results at this tail speed are included.

Eight metrics were evaluated to determine the effects of the aerodynamic tail on *AeroDima*. These metrics, illustrated in Fig. 12, were: (1) the average and (2) maximum linear acceleration, (3) the average and (4) maximum yaw rate, (5) the average and (6) maximum maneuvrability metric, (7) the roll rate stability of the vehicle, and (8) the top vehicle speed achieved during turning [3] [10] [15] [16] [17]. The maneuvrability metric is given by the forward velocity multiplied by the yaw rate as seen in the formula:

$$K = \dot{\theta} v \tag{2}$$

The simulated and experimental results from the fastest runs for each configuration are given in Table I. Footage of the experiments is shown in Fig. 11. These same runs can be seen in the accompanying video. The tailless *AeroDima* can be seen toppling over at a speed at which the tailed version of the platform comfortably executes the turning maneuver.

VI. Discussion and Conclusion

Despite modeling the ground as a smooth surface in simulations, our findings closely align with physical tests conducted on grass for all metrics except the combined maneuverability metric, where the tailed configuration outperformed its simulation counterpart. The introduction of an aerodynamic tail significantly enhances stability, demonstrated by a marked reduction in roll rate, enabling the robot to initiate turns at increased speeds without the risk of toppling. Interestingly, the reduction in yaw rate and lateral acceleration suggests that the tail's primary contribution to maneuverability stems from improved stability rather than

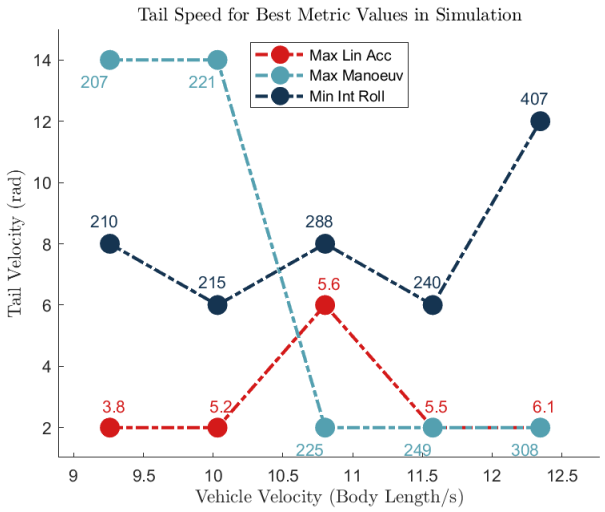

Fig. 13: The best tail flick speeds per forward velocity for the max linear acceleration, max maneuvrability, and integral of roll rate.

directly facilitating quicker turns, corroborating our earlier work on the role of free appendages in maneuverability [18].

The implementation of an aerodynamic tail raised the platform's maximum turning speed from 3.27 m/s to 6.1 m/s, an 87% improvement. Although this increase falls short of the 142% enhancement seen with the original *Dima* platform's inertial tail [3], it's important to note the aerodynamic tail constitutes only 1.5% of *AeroDima's* mass—significantly lighter compared to the inertial tail's 8%. However, comparisons are nuanced due to *AeroDima's* increased weight, height, and power.

A notable study limitation is the application of simple open-loop control, with the tail flicked at a constant velocity, irrespective of the robot's speed. Varied tail speeds in simulations indicated optimal speeds change with the robot's velocity (Fig. 13), suggesting a passive role for the tail at higher speeds. Future work will delve deeper into aerodynamic tail control and enhancing sensor accuracy, particularly GPS, to refine the interplay between inertial and aerodynamic tail effects. We also aim to extend our lightweight tail design across diverse robotic platforms, assessing its scalability and performance impact.

Acknowledgment

The authors would like to Mathworks for their generous support of this research.

References

[1] N. C. Sharp, "Timed running speed of a cheetah (Acinonyx jubatus)," *Journal of Zoology*, vol. 241, no. 3, pp. 493–494, 3 1997.

[2] J. W. Wilson, M. G. Mills, R. P. Wilson, G. Peters, M. E. Mills, J. R. Speakman, S. M. Durant, N. C. Bennett, N. J. Marks, and M. Scantlebury, "Cheetahs, Acinonyx jubatus, balance turn capacity with pace when chasing prey," *Biology Letters*, vol. 9, no. 5, 9 2013.

[3] A. Patel and M. Braae, "Rapid turning at high-speed: Inspirations from the cheetah's tail," *IEEE International Conference on Intelligent Robots and Systems*, pp. 5506–5511, 2013.

[4] ——, "Rapid acceleration and braking: Inspirations from the cheetah's tail," in *2014 IEEE International Conference on Robotics and Automation (ICRA)*. IEEE, 2014, pp. 793–799.

[5] A. Patel, E. Boje, C. Fisher, L. Louis, and E. Lane, "Quasi-steady state aerodynamics of the cheetah tail," *Biology Open*, vol. 5, no. 8, pp. 1072–1076, 2016.

[6] J. Zhao, T. Zhao, N. Xi, M. W. Mutka, and L. Xiao, "MSU Tailbot: Controlling Aerial Maneuver of a Miniature-Tailed Jumping Robot," *IEEE/ASME Transactions on Mechatronics*, vol. 20, no. 6, pp. 2903–2914, 12 2015.

[7] R. Briggs, J. Lee, M. Haberland, and S. Kim, "Tails in biomimetic design: Analysis, simulation, and experiment," in *IEEE International Conference on Intelligent Robots and Systems*, 2012, pp. 1473–1480.

[8] E. Chang-Siu, T. Libby, M. Tomizuka, and R. J. Full, "A lizard-inspired active tail enables rapid maneuvers and dynamic stabilization in a terrestrial robot," *Institute of Electrical and Electronics Engineers (IEEE)*, pp. 1887–1894, 12 2011.

[9] J. Norby, J. Y. Li, C. Selby, A. Patel, and A. M. Johnson, "Enabling Dynamic Behaviors With Aerodynamic Drag in Lightweight Tails," *IEEE Transactions on Robotics*, pp. 1–10, 2021.

[10] N. J. Kohut, A. O. Pullin, D. W. Haldane, D. Zarrouk, and R. S. Fearing, "Precise dynamic turning of a 10 cm legged robot on a low friction surface using a tail," in *Proceedings - IEEE International Conference on Robotics and Automation*, 2013, pp. 3299–3306.

[11] C.E.Brennen, "A review of added mass and fluid inertial forces," Naval Civil Engineering Laboratory, California, Tech. Rep. January, 1982.

[12] E. J. Grift, N. B. Vijayaragavan, M. J. Tummers, and J. Westerweel, "Drag force on an accelerating submerged plate," *Journal of Fluid Mechanics*, vol. 866, pp. 369–398, 2019.

[13] S. Hoerner, "Fluid-dynamic drag: practical information on aerodynamic drag and hydrodynamic resistance," *Journal of Physics: Conference Series*, vol. 75, pp. 1–455, 1965.

[14] M. Huang, W. Wang, and J. Li, "Analysis and verification of aerodynamic characteristics of tianwen-1 mars parachute," *Space: Science and Technology*, vol. 2022, 1 2022.

[15] A. Patel and E. Boje, "On the conical motion of a two-degree-of-freedom tail inspired by the cheetah," *IEEE Transactions on Robotics*, vol. 31, pp. 1555–1560, 12 2015.

[16] N. J. Kohut, D. Zarrouk, K. C. Peterson, and R. S. Fearing, "Aerodynamic steering of a 10 cm high-speed running robot," *IEEE International Conference on Intelligent Robots and Systems*, pp. 5593–5599, 2013.

[17] A. McClung, "Techniques for dynamic maneuvering of hexapedal legged robots," Ph.D. dissertation, Stanford University, 2006.

[18] S. Shield, R. Jericevich, A. Patel, and A. Jusufi, "Tails , flails and sails : How appendages improve terrestrial maneuverability by improving stability," *Integrative & Comparative Biology*, pp. 1–12, 2021.